

The following resources related to this article are available online at www.sciencemag.org (this information is current as of November 24, 2009):

Updated information and services, including high-resolution figures, can be found in the online version of this article at:

<http://www.sciencemag.org/cgi/content/full/288/5465/475>

This article has been **cited by** 196 article(s) on the ISI Web of Science.

This article has been **cited by** 4 articles hosted by HighWire Press; see:

<http://www.sciencemag.org/cgi/content/full/288/5465/475#otherarticles>

This article appears in the following **subject collections**:

Physics

<http://www.sciencemag.org/cgi/collection/physics>

Information about obtaining **reprints** of this article or about obtaining **permission to reproduce this article** in whole or in part can be found at:

<http://www.sciencemag.org/about/permissions.dtl>

Quantum Criticality: Competing Ground States in Low Dimensions

Subir Sachdev

Small changes in an external parameter can often lead to dramatic qualitative changes in the lowest energy quantum mechanical ground state of a correlated electron system. In anisotropic crystals, such as the high-temperature superconductors where electron motion occurs primarily on a two-dimensional square lattice, the quantum critical point between two such lowest energy states has nontrivial emergent excitations that control the physics over a significant portion of the phase diagram. Nonzero temperature dynamic properties near quantum critical points are described, using simple theoretical models. Possible quantum phases and transitions in the two-dimensional electron gas on a square lattice are discussed.

Quantum mechanics was originally developed by Schrödinger and Heisenberg as a theory of nonrelativistic charged particles interacting via the Coulomb force, and successfully applied to a simple two-particle system like the hydrogen atom. However, among its most important applications has been the description of $\sim 10^{23}$ particles found in macroscopic matter. The earliest example of this was the Sommerfeld-Bloch theory of electronic motion in metals, and its refined formulation in Landau's Fermi liquid theory (1). Although solving Schrödinger's wave equation for 10^{23} interacting electrons appears an impossibly daunting task, Landau outlined a powerful strategy, involving the concept of "quasiparticles," which allowed an essentially exact description of the low-temperature (T) properties of metals. Extensions of Landau's approach have successfully described many other phases of matter: the superfluid phases of ^4He and ^3He , the superconductivity in metals that is described by the Bardeen-Cooper-Schrieffer theory, and the quantum Hall liquid state of electrons in two dimensions in a strong magnetic field. However, in the last decade, attention has been lavished on new transition metal compounds for which no successful quasiparticle-like theory has yet emerged for much of the accessible temperature range. The most important among these compounds are ceramics, like $\text{YBa}_2\text{Cu}_3\text{O}_7$, in which the electronic motion occurs primarily in two-dimensional (2D) CuO_2 layers, and that display "high-temperature" superconductivity.

Here, I shall describe a new approach to the collective dynamical properties of electrons that turns out to be especially useful in two dimensions: the approach focuses on the notion of competing ground states and its

implications for the dynamics of excited states at nonzero temperatures. Before describing this further, let us review the essence of Landau's strategy. His starting point is the proper identification of the quantum "coherence" or order in the ground state of the system. In the theory of metals, the order is that implied by the distribution in the occupation number of plane wave states of electrons—the plane waves with small wavevectors are fully occupied, but there is an abrupt decrease in the average occupation number above a certain "Fermi wavevector"; in the superfluid state of ^4He , the order in the ground state is the presence of the Bose-Einstein condensate—the macroscopic occupation of ^4He atoms in the ground state. Landau then proceeds to describe the low-energy excited states, and hence the finite temperature properties, by identifying elementary excitations that perturb the order of the ground state in a fundamental way. These excitations can be thought of as new, emergent particles (or "quasiparticles") that transport spin, charge, momentum, and energy, and whose mutual collisions are described by a Boltzmann-like transport equation. In metals, the quasiparticles are electrons and holes in the vicinity of the Fermi wavevector, whereas in ^4He they are phonon and roton excitations.

The systems I shall consider here are delicately poised between two or more distinct states with very different quantum ordering properties and low-lying excitations. The energies of the states are quite close to each other, and only at very low temperatures is a particular one picked as the ground state—at these temperatures, Landau's quasiparticle approach can apply. However, for somewhat different parameters, it is possible that a different state will be picked as ground state, and again, Landau's quasiparticle approach will apply at very low temperatures: a crucial point is that the nature and physical proper-

ties of these quasiparticles will, in general, be very different from the previous ones. At slightly higher temperatures, it is impossible to ignore the competition between the different states and their respective quasiparticles: the simple quasiparticle picture breaks down, and very complex behavior can result which is not characteristic of any one of the possible ground states.

I describe this intricate temperature dependence by the following strategy. Imagine following the true ground state of the system as a function of some parameter in the Hamiltonian, g . It should be possible to find a critical value $g = g_c$ such that the ground state undergoes a quantum phase transition (2, 3) from one possible state for $g < g_c$ to another, with distinct quantum order, for $g > g_c$. I first develop a theory for the ground state for the quantum critical point precisely at $g = g_c$. In general, this is a difficult task, but for "second-order" quantum transitions, the critical point has special symmetry properties that often allows significant progress; we will see examples of this below. Empowered with this knowledge of the physics at intermediate coupling, I move away from the critical point and map out the physics for nonzero $|g - g_c|$ and temperature. It should be emphasized that it is often the case that the point $g = g_c$ is in a regime that cannot be experimentally accessed; however, this does not rule out application of my strategy—it is still useful to describe the physics at the inaccessible point $g = g_c$, and then use it as a point of departure to develop a systematic and controlled theory for an accessible value of g .

This discussion has so far been rather abstract; we will now spell out concrete details by considering a number of examples of increasing complexity and discussing their relationship to experimental observations.

Ising Chain in a Transverse Field

This is the simplest theoretical model of a quantum phase transition, and many key concepts emerge from its study (3). It is described by the Hamiltonian ($J > 0$, $g > 0$)

$$H_I = -J \sum_j (g \hat{\sigma}_j^x + \hat{\sigma}_j^z \hat{\sigma}_{j+1}^z) \quad (1)$$

Here, $\hat{\sigma}_j^{x,z}$ are Pauli matrices that measure the x, z components of the electron spin on a magnetic ion in an insulator. The ions reside on the sites j of a 1D chain. Each site has two possible states $|\uparrow\rangle_j$ and $|\downarrow\rangle_j$, which are ei-

Department of Physics, Yale University, Post Office Box 208120, New Haven, CT 06520-8120, USA.

E-mail: subir.sachdev@yale.edu; URL: <http://pantheon.yale.edu/~subir>

genstates of $\hat{\sigma}_j^z$ with eigenvalues $+1$ and -1 , and thus identify the electron spin on site j as “up” or “down.” The two terms in H_1 represent different physical effects: the second term prefers that the spins on neighboring ions are parallel to each other, whereas the first allows quantum tunneling between the $|\uparrow\rangle_j$ and $|\downarrow\rangle_j$ states with amplitude proportional to g .

For $g \gg 1$ and for $g \ll 1$, the ground states of H_1 are simple, and the quasiparticle picture does describe the low T dynamics (4). For $g \ll 1$, we can neglect the quantum tunneling and the ground state either has all spins up or all spins down. The order in this state is evident: all the spins are parallel to each other. The quasiparticles are domain walls that perturb this order. A quasiparticle state, $|\mathcal{Q}_j\rangle$, between sites j and $j+1$ has the following wavefunction: all spins at and to the left (right) of site j ($j+1$) are up (down) (see Fig. 1). For $g = 0$, every such spin configuration is an energy eigenstate and therefore stationary; for small but finite g , the domain walls become mobile (and acquire zero point motion). A theory for the quantum kinetics of these particles, describing their collisions, lifetime, and the relaxation of the magnetic order, can be developed following Landau’s general strategy. In the opposite limit, $g \gg 1$, we see from Eq. 1 that the ground state can be built out of eigenstates of $\hat{\sigma}_i^x$ with eigenvalue $+1$: these are

$$|\rightarrow\rangle_j = \frac{1}{\sqrt{2}} (|\uparrow\rangle_j + |\downarrow\rangle_j) \quad (2)$$

or a “right”-pointing spin, which quantum mechanically is just a linear superposition of up and down spins. The ground state has all spins pointing to the right, and it is evident that such a state is very different from the $g = 0$ ground state, because the two states form distinct quantum superpositions of the avail-

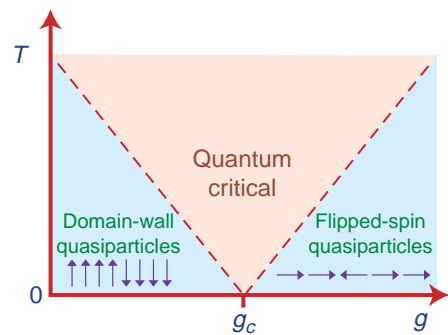


Fig. 1. Phase diagram of H_1 . The quantum phase transition is at $g = g_c$, $T = 0$, and the dashed red line indicates a crossover. Quasiparticle dynamics applies in the blue shaded regions: for $g < g_c$, the quasiparticle states are like the $|\mathcal{Q}_j\rangle$ states, whereas for $g > g_c$, they are like the very different $|\tilde{\mathcal{Q}}_j\rangle$ states. The quantum critical dynamics in the pink shaded region is characterized by Eq. 5.

able states in the Hilbert space. The distinction extends also to the excited states: we define a left-pointing spin by the analog of (2), $|\leftarrow\rangle_j = (|\uparrow\rangle_j - |\downarrow\rangle_j)/\sqrt{2}$, and the quasiparticle states, $|\tilde{\mathcal{Q}}_j\rangle$, now represent a single “left”-pointing spin at site j in a background of “right” spins (see Fig. 1), rather than a domain wall. For $g = \infty$, these states are stationary, but for $g < \infty$, the quasiparticles develop dynamics; a theory for this dynamics can again be formulated in the spirit of Landau, and this describes relaxation phenomena at low T .

We now allow competition between the distinct orders at small and large g by considering values of g of order unity. Consider first $T = 0$. It is known that there is a quantum phase transition between these states at $g = g_c = 1$, i.e., the ground state qualitatively similar to the $g = 0$ ground state for all $g < 1$, while a state like the $g = \infty$ ground state is favored for $g > 1$. The ground state precisely at $g = g_c$ is very special: it cannot be characterized by any such simple cartoon pictures. Its fundamental property is one of scale invariance, as is apparent from the ground state correlation function (5)

$$\langle \hat{\sigma}_j^z \hat{\sigma}_k^z \rangle \sim \frac{1}{|j - k|^{1/4}} \quad \text{for large } |j - k| \quad (3)$$

This power-law decay has the property that the functional form of the correlation is only modified by an overall prefactor if we stretch the length scale (i.e., perform a scale transformation) at which we are observing the spins. In other words, it is not possible to tell by an examination of the ground state wavefunction how far apart any pair of well-separated spins are. At $T > 0$, a new time scale does appear, namely $\hbar/k_B T$, and a fundamental property of the quantum critical point of H_1 is that this time scale (involving nothing but the temperature and fundamental constants of nature) universally determines the relaxation rate for spin fluctuations. This is made more precise by examining the zero-momentum dynamic response function

$$\chi(\omega) = \frac{i}{\hbar} \sum_k \int_0^\infty dt [(\hat{\sigma}_j^z(t), \hat{\sigma}_k^z(0))] e^{i\omega t} \quad (4)$$

where $\hat{\sigma}_j^z(t)$ is an operator at time t in the Heisenberg picture, and $[\cdot, \cdot]$ represents a quantum commutator. The arguments above and simple dimensional considerations following from Eq. 3 imply that for low temperatures χ obeys

$$\chi(\omega) \sim T^{-7/4} \Phi_1(\hbar\omega/k_B T) \quad (5)$$

with Φ_1 a universal response function; if, for example, we added a small second neighbor coupling to H_1 , the critical coupling g_c would shift slightly but Φ would remain exactly the same. The exact result for Φ_1 is known, and it is an excellent approximation to just replace

its inverse by a low-frequency expansion (3) $\Phi_1(\hbar\omega/k_B T) = A(1 - i\omega/\Gamma_R + \dots)^{-1}$; here, A is a dimensionless prefactor, and we have the important result that $\Gamma_R = [2 \tan(\pi/16)]k_B T/\hbar$. This is the response of an overdamped oscillator with a relaxation rate determined only by temperature itself (6). Although a quasiparticle description of this response function is strictly not possible, we can visualize the dynamics in terms of a dense gas of the $|\mathcal{Q}_j\rangle$ particles scattering off each other at a rate of order $k_B T/\hbar$; however, a picture in terms of the “dual” $|\tilde{\mathcal{Q}}_j\rangle$ particles would also be valid. It is quite remarkable that the strength of the underlying exchange interaction between the spins does not appear in these fundamental dynamic scales.

We can use these above results to sketch a crossover phase diagram in the g, T plane. This is shown in Fig. 1. Note that “quantum criticality,” characterized by responses like Eq. 5, holds over a range of values of g at nonzero temperature (7).

It can be shown that the physics of the quantum Ising model in spatial dimension $d = 2$ is very similar; quantum criticality is again characterized by Eq. 5 (but the exponent $7/4$ is replaced by a different universal numerical value). Similar behavior applies also to quantum transitions in $d = 3$ systems with quenched disorder (8). However, for the analog of H_1 in $d = 3$ (and for all $d > 3$), the physics of the quantum phase transition is very different (3)—the kinetic theory of the analog of the $|\tilde{\mathcal{Q}}_j\rangle$ quasiparticles applies even at the critical point, and their scattering cross-section depends on the magnitude of the microscopic interactions. Quantum transitions in this class have been studied elsewhere and have important physical applications (9–11): our discussion of quantum criticality will not apply to them.

Coupled Ladder Antiferromagnet

We turn to a model in $d = 2$ that is indirectly related to microscopic models of the high temperature superconductors. We consider the antiferromagnet described by the Hamiltonian (12) ($J > 0$, $0 < g \leq 1$)

$$H_L = J \sum_{i,j \in A} \mathcal{S}_i \cdot \mathcal{S}_j + gJ \sum_{i,j \in B} \mathcal{S}_i \cdot \mathcal{S}_j \quad (6)$$

where \mathcal{S}_i are spin-1/2 operators on the sites of the coupled-ladder lattice shown in Fig. 2, with the A links forming “two-leg ladders” while the B links couple the ladders. There is a quantum phase transition in H_L at a critical value $g = g_c \approx 0.3$ that is similar in many respects to that in H_1 .

I begin by describing the well-ordered ground states on either side of g_c and their respective, low- T quasiparticle theories.

For g close to unity, there is the magnetically ordered “Néel” state in Fig. 2A. This is analogous to the ground state of H_1 for small

g , with the difference that the mean moment on the sites has a staggered sublattice arrangement. There is also an important difference in the structure of the excitations, because H_L has the symmetry of arbitrary rotations in spin space, in contrast to the discrete spin inversion symmetry of H_T . Consequently, the low-lying quasiparticle excitations are spin waves corresponding to a slow precession in the orientation of the staggered magnetic order. The precession can be either clockwise or anticlockwise, and so there is twofold degeneracy to each spin-wave mode. Because of infrared singular scattering of thermally excited spin waves in $d = 2$, the theory of spin-wave dynamics has some subtleties (7, 13); nevertheless, the results remain within the spirit of the quasiparticle picture.

For small g , the ground state is a quantum paramagnet, and a caricature is sketched in Fig. 2B. The average moment on each site has been completely quenched by the formation of singlet bonds between neighboring spins. This state is similar in many respects to the large g ground state for H_T . It requires a finite energy, Δ , to create quasiparticle excitations by locally disrupting the singlet order (the analog of flipping a spin for H_T): the singlet bond between a pair of spins can be replaced by a triplet of total spin $S = 1$ states, and the motion of this broken bond corresponds to a threefold degenerate quasiparticle state (to be contrasted with the twofold degenerate spin wave above). A conventional quantum Boltzmann equation can be used to describe the low temperature dynamics of these triplet quasiparticles (3, 14).

The crossover phase diagram in the g, T plane (7) is sketched in Fig. 3 following Fig. 1. For $g \leq g_c$, quantum criticality appears for $\Delta \ll k_B T \ll J$. Here, dynamic spin response

functions have a structure very similar to that described near Eq. 5: the relaxation rate Γ_R continues to be proportional to $k_B T/\hbar$, but now only approximate results for the proportionality constant are available (3, 15). If the dynamics is described in the basis of the triplet quasiparticles, then these results imply that the scattering cross section is universally determined by the energy $k_B T$ alone (14). As we lower $k_B T$ across Δ (for $g < g_c$), this scattering cross section evolves as a function of the dimensionless ratio $\Delta/k_B T$ alone, and for very low T is determined by Δ alone. One remarkable consequence of this universal cross section is that transport coefficients, like the spin conductance σ_s (which determines the spin current produced by the gradient in an applied magnetic field), are determined by fundamental constants of nature (16) and the ratio $\Delta/k_B T$

$$\sigma_s = \frac{(g\mu_B)^2}{h} \Phi_\sigma \left(\frac{\Delta}{k_B T} \right) \quad (7)$$

Here, g is the gyromagnetic ratio of the ions carrying the spin, μ_B is the Bohr magneton, and Φ_σ is a universal function with no arbitrariness in either its overall scale or in that of its argument. Note that, well into the quantum critical region, σ_s is proportional to the universal number $\Phi_\sigma(0)$, and so is determined by constants of nature alone.

Although it is certainly not appropriate to take H_L as a literal model for the high-temperature superconductors, it is notable (17) that many measurements of spin fluctuations in the last decade display crossovers that are very similar to those found in the vicinity of the quantum critical point in Fig. 3. I take this as evidence that the high-temperature superconductors are near a quantum critical point whose spin sector has universal properties

closely related to that of H_L (18): a specific microscopic calculation, involving competition between the states to be discussed below, which realizes such a scenario was presented in (19). The evidence has appeared in the following experiments: (i) the dynamic spin structure factor measured in neutron scattering experiments (20) at moderate temperature obeys scaling forms similar to Eq. 5; (ii) as I discuss in Fig. 4, crossovers in the nuclear spin relaxation rate (21, 24, 25) as a function of carrier density and temperature match very well with the spin dynamics of the different regimes in the g, T plane in Fig. 3; (iii) low-temperature neutron scattering measurements (26) at higher carrier density show a resolution-limited peak above a finite energy gap; this is a signal of the long-lived triplet quasiparticles, like those found at low T for $g < g_c$ in H_L ; such a peak was argued early on (15) to be a generic property of the vicinity of a quantum critical point, like that in H_L , proposed for the high-temperature superconductors (18). A further test of quantum criticality in the spin fluctuations could be provided by measurements of the spin conductance and comparison with Eq. 7, but such experiments have not been feasible so far.

Electronic Ground States in Two Dimensions

I have so far discussed simple models of quantum phase transitions whose physics is now well understood. Here, I turn to more realistic models of the high-temperature superconductors. As I mentioned in the intro-

Fig. 2. The coupled ladder antiferromagnet; the spin-1/2 degrees of freedom, S_i , reside on the blue circles. The A links are the full red lines and have exchange J , whereas the B links are dashed lines and have exchange gJ . The Néel ground state for $g > g_c$ appears in (A). The paramagnetic ground state for $g < g_c$ is schematically indicated in (B). The ellipses in (B) represents a singlet valence bond, $(|\uparrow\downarrow\rangle - |\downarrow\uparrow\rangle)/\sqrt{2}$ [shown in (C)], between the spins on the sites.

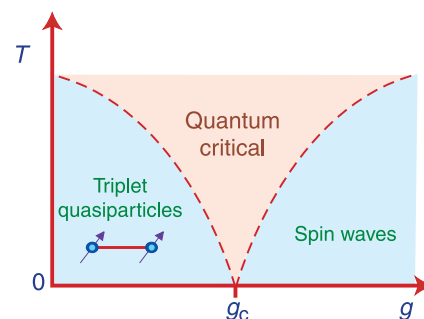
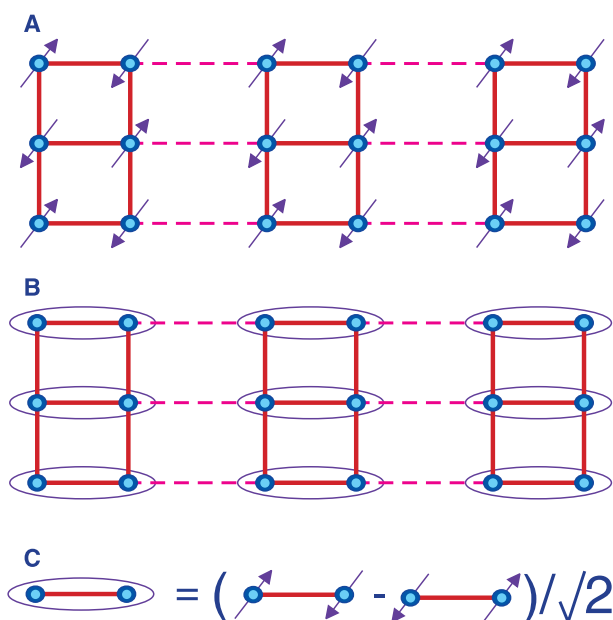


Fig. 3. Crossover phase diagram for H_L with the same conventions as Fig. 1. The ground state is a paramagnet (Fig. 2B) for $g < g_c$, and the energy cost to create a spin excitation, Δ , is finite for $g < g_c$ and vanishes as $\Delta \sim (g_c - g)^{z\nu}$, where $z\nu$ is a critical exponent. There is magnetic Néel order at $T = 0$ for $g > g_c$ (Fig. 2A), and the time-averaged moment on any site, \bar{N}_i , vanishes as g approaches g_c from above. Quasiparticle-like dynamics applies in the blue-shaded regions. For $g < g_c$, in the cartoon picture of the ground state in Fig. 2B, the triplet quasiparticle corresponds to the motion of broken singlet bond in which Fig. 2C is replaced by one of $|\uparrow\uparrow\rangle$, $|\downarrow\downarrow\rangle$, or $(|\uparrow\downarrow\rangle + |\downarrow\uparrow\rangle)/\sqrt{2}$. For $g > g_c$, the quasiparticles are spin-waves representing slow, long-wavelength deformations of the ordered state in Fig. 2A.

duction, electronic motion in these materials occurs primarily in 2D CuO_2 layers. The Cu ions are located on the vertices of a square lattice, and it is widely believed that only the dynamics on a single 3d Cu orbital is relevant, with the occupation numbers of the other orbitals being inert. So we are led to consider a simple tight-binding model of electrons with a single orbital on every site of a square lattice, along with Coulomb interactions between the electrons. If the electron density is precisely unity per site, then the ground state is known to be an insulator with Néel order (this corresponds to the state in Fig. 2A at $g = 1$) for the range of parameters found in the stoichiometric compound La_2CuO_4 . It is possible to vary the electron density in the square lattice by doping such a compound to $\text{La}_{2-x}\text{Sr}_x\text{CuO}_4$, and then x measures the density of holes relative to the insulating state with one electron per site. High-temperature superconductivity is found for x greater than about 0.05.

Much theoretical work in the last decade has addressed the physics of this square lattice model for small x . I will discuss various proposals for ground states, with an emphasis on finding sharp distinctions between them—i.e., distinguishing states that cannot be smoothly connected by the variation of a parameter in the Hamiltonian and that must

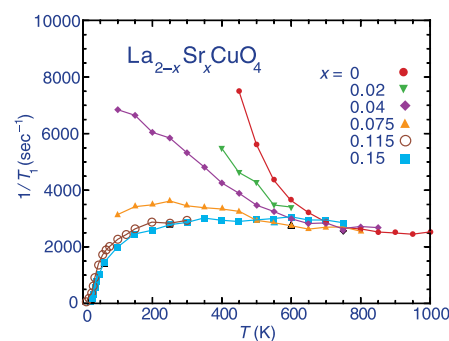


Fig. 4. Measurements (21) of the longitudinal nuclear spin relaxation ($1/T_1$) of ^{63}Cu nuclei in the high-temperature superconductor $\text{La}_{2-x}\text{Sr}_x\text{CuO}_4$ as a function of x and T . This quantity is a measure of the spectral density of electron spin fluctuations at very low energies. At small x , $1/T_1$ increases rapidly as T is lowered (red circles). This is also the behavior in the spin-wave regime of Fig. 3 ($g > g_c$): the energy of the dominant thermally excited spin-wave decreases rapidly as T decreases, and so the spin spectral density rises (22). In contrast, at large x , $1/T_1$ decreases as T is lowered (blue squares). This corresponds with the triplet quasiparticle regime of Fig. 3 ($g < g_c$): the low-energy spectral density is proportional to the density of thermally excited quasiparticles, and this becomes exponentially small as T is lowered. Finally, at intermediate T , $1/T_1$ is roughly temperature-independent for a wide range of T (orange triangles), and this is the predicted behavior (18, 23) in the quantum critical regime of Fig. 3.

be separated by a quantum phase transition. Often, the theoretical debate has been about different approximation schemes to computing properties of states that are ultimately equivalent. I avoid such issues here; indeed, I advocate that a sound approach is to use a theory for quantum critical points, separating distinct ground states, to develop a controlled expansion at intermediate coupling.

A minimal approach to identifying possible ground states is to assume that they are fully characterized by broken symmetries of the underlying Hamiltonian—i.e., a simple electron mean-field theory of the broken symmetry properly identifies the elementary excitations (however, as discussed above, this does not rule out highly nontrivial quantum critical points whose excitations control the physics over a wide region of the phase diagram). The symmetries that leave the Hamiltonian invariant (and so may be broken by the ground state) are time-reversal, the group of spin rotations, the space group of the square lattice, and the electromagnetic gauge symmetry related to charge conservation. Even in this limited framework, the possibilities are remarkably rich, and it is entirely possible that they will provide an explanation for all

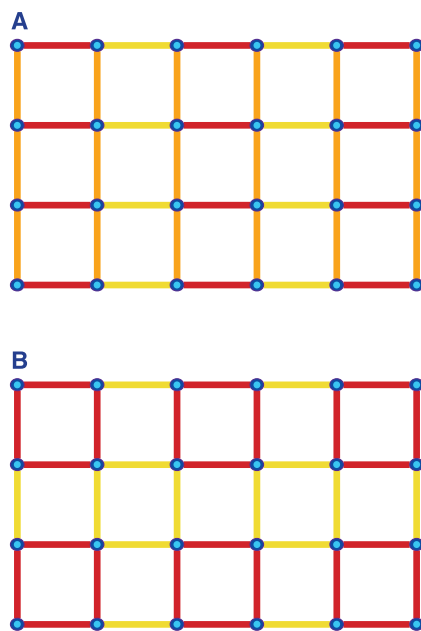


Fig. 5. Two examples (A and B) of square lattice ground state with Peierls order. All sites are equivalent, and distinct values of the energy and charge densities on the links are represented by distinct colors. These distinctions represent a spontaneous breaking of the symmetry of the square lattice space group. The spontaneous ordering appears because it optimizes the energy gained by resonance between different singlet bond pairings of near-neighbor spins. This figure should be contrasted with Fig. 2, where there is no spontaneous breaking of translational symmetry, and the distinction between the links is already present in the Hamiltonian Eq. 6.

the experiments. More exotic ground states have also been proposed, and I will note them briefly below.

One important state has already made an appearance in the discussion above, and is known to be the ground state $x = 0$: the Néel state sketched in Fig. 2A. It is apparent by a glance at the staggered arrangement of spins in Fig. 2A that we can view this state as a density wave of spin polarization at the wavevector $\mathbf{K} = (\pi/a, \pi/a)$, where a is the square lattice spacing. For small $x \neq 0$, spin density waves with a period incommensurate with the underlying lattice have been observed (27): these states have a mean spin polarization at a wavevector \mathbf{K} that varies continuously away from $(\pi/a, \pi/a)$.

The other ground state of central importance is, of course, the superconducting state. This is formed by Bose condensation of electrons in Cooper pairs, which leads to the breaking of the electromagnetic gauge symmetry. It is known that the pair wavefunction has the symmetry of the $d_{x^2-y^2}$ orbital in the relative coordinate of the two electrons. Recently, interest has focused on the question of whether the pair wavefunction is on the verge of acquiring an additional imaginary component with d_{xy} (or possibly s) symmetry: such an instability would also break time-reversal symmetry (28–31). It has been argued (31) that the quantum phase transition between two such superconductors could very naturally explain the quantum criticality, similar to the scaling form (5), observed in recent photoemission experiments (32).

A state that makes a frequent appearance in theoretical studies is one with “Peierls” order. In models with half-integral spin per unit cell, such order was argued (33) to be a generic property of any state reached by a continuous quantum transition that restores the broken spin rotation symmetry of a Néel state. The Peierls order is associated with broken translational symmetries, and examples are shown in Fig. 5: in these states all sites of the square lattice are equivalent, but links connecting nearest neighbor sites spontaneously can acquire distinct values for their charge and energy densities (and therefore, for the mean value of the exchange coupling $\langle \mathbf{S}_i \cdot \mathbf{S}_j \rangle$). I also considered a quantum transition restoring spin rotation symmetry previously in the text, and mentioned its relevance to the NMR measurements in Fig. 4; however, the issue of spontaneous Peierls ordering did not arise there because the links were already explicitly inequivalent in the Hamiltonian H_L in Eq. 6. It is believed (15, 33, 34) that the universal spin fluctuation properties in the vicinity of the quantum critical point discussed above apply also to cases where spontaneous Peierls order appears in the paramagnetic state. Evidence for the spontaneous Peierls ordering in Fig. 5A has

emerged in numerical studies (35, 36) of square lattice models at $x = 0$ and with first- and second-neighbor hopping of electrons, and also in nearest-neighbor hopping models for $x > 0$ (37).

A competitor state to Peierls order for the quantum paramagnet is the “orbital antiferromagnet” (38–40): this state breaks time-reversal and translational symmetries, but spin rotation symmetry and the combination of time-reversal and translation by an odd number of lattice spacings remains unbroken. There is a spontaneous flow of electrical currents around each plaquette of the square lattice, with clockwise and anticlockwise flows alternating in a checkerboard pattern (Fig. 6). Ivanov *et al.* (41) proposed that a closely related state (in their formulation, there are strong fluctuations of the orbital currents, but no true long-range order) is responsible for the “pseudo-gap” phenomenology of the high-temperature superconductors—the pseudo-gap is the partial quenching of low-energy spin and fermionic excitations at temperatures above the superconducting critical temperature (T_c).

For the final conventional state, I consider a charge density wave. Much recent experimental work has centered around the discovery of charge-ordering in certain high-temperature superconductors and related materials (42). An especially stable state, observed for $x \approx 1/8$, has a charge density wave at wavevector $\mathbf{K} = [\pi/(2a), 0]$; depending upon its phase, the charge density wave can be either site-centered or bond-centered, as shown in Fig. 7. Current experiments do not distinguish between these two possibilities. Site-centered ordering was considered in some early theoretical work (43–45), although with a very different charge distribution than is now observed. Bond-centered ordering was considered recently (19, 46, 47), and has some attractive features: it enhances singlet-bond formation between spins, optimizing the energy gained through quantum fluctuations in an antiferromagnet, and so is preferred by the same effects that led to the Peierls ordering in Fig. 5. Also, bond-centering is naturally compatible with the observed coexistence of charge-ordering and superconductivity at lower temperatures (48), while site-centering is expected to lead to insulating behavior. Let me also mention that superposition of charge density waves with different noncollinear \mathbf{K} can lead to an insulating Wigner crystal state; this could be a Wigner crystal of holes, or with an even number of particles per unit cell, a Wigner crystal of Cooper pairs (47).

Clearly, a fascinating variety of phase diagrams and quantum phase transitions are possible among the states I have discussed above. In principle, many of the order parameters can coexist with each other, and this

adds to the menagerie of possibilities. Future experiments with increased sensitivity should make it possible to more clearly detect more of these orderings, and thus select between various scenarios.

Spin-Charge Separation

Finally, we discuss more exotic possibilities of states that cannot be completely characterized by ordering discussed above. Of particular interest has been the early proposal of Anderson and others (49, 50) that there could be an insulating state with spin-charge separation; i.e., the electron falls apart (“fractionalizes”) into separate deconfined excitations (51, 52) that carry its spin and charge. A fundamental property of these deconfined phases is that superconducting states in their vicinity allow low-energy vortex excitations with quantized magnetic flux equal to hc/e (53–55): the elementary flux quantum is always $hc/2e$, but it can be argued quite generally that core energy of a hc/e vortex is lower than twice that of a $hc/2e$ vortex. The kinetic energy of the superflow well away from the vortex core always prefers the smaller flux $hc/2e$, and so requiring global stability for hc/e vortices becomes a delicate question of balancing core and superflow contributions (53). Nevertheless, it is possible, in principle, that a magnetic flux decoration, flux noise, tunneling, or other experiment could observe metastable or stable hc/e vortices or vortex-antivortex pairs: this would be a “smoking-gun” signal for deconfinement.

Another important class of experiments (56) measures the response to nonmagnetic impurities, such as Zn or Li, and these could also provide clear-cut answers on the nature of the order parameter and on issues of confinement. These impurities substitute on the Cu site and so are directly within the plane of the 2D electron gas. Such deformations are very effective in disrupting the quantum coherence of the ground state and so serve as effective probes of its structure. For example (57, 58), replacing only 0.5% of Cu by Zn dramatically broadens the peak in the neutron-

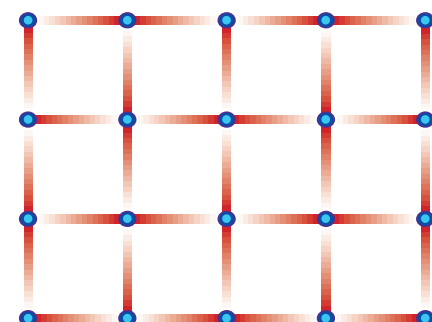


Fig. 6. The orbital antiferromagnet. The gradient in the red shading represents the direction of spontaneous current flow on the links, which breaks time-reversal symmetry.

scattering cross section (26), arising from the triplet quasiparticles discussed above. Further interesting developments are sure to follow.

Conclusion

Correlated electron systems in two dimensions are in a privileged position. Those in three dimensions either form good Fermi liquids or ordered states with order parameters like those discussed above: in the latter case, quantum fluctuations of the order parameter are weak and do not lead any unusual non-quasiparticle behavior, even at zero temperature phase transitions (11). In contrast, in one dimension, quantum fluctuations of the order parameters are so strong that they usually preclude the emergence of long-range order, and so quantum phase transitions are harder to find. It is in two dimensions that there is a delicate balance between order and fluctuation, and a host of interesting quantum critical points, with nontrivial universal properties, can appear between different competing orders. I have considered some simple examples of the dynamical properties of systems near such a point. The phases on either side of the critical point are usually amenable to a quasiparticle description at low enough temperatures. However, a key point is that the quasiparticle states are very different for the two phases, so at slightly higher temperatures

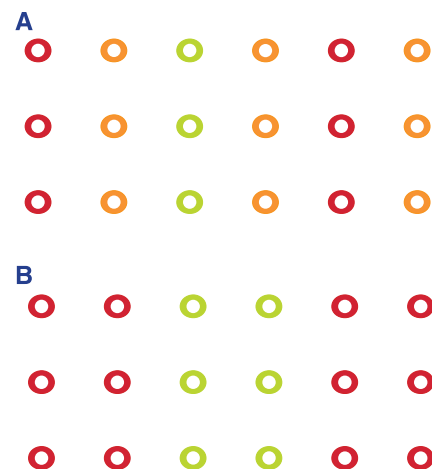


Fig. 7. Charge density waves with (A) site- and (B) bond-centering; both states have a 4×1 unit cell. The state in (A) is symmetric about reflections in a vertical axis running through the red or green sites, whereas that in (B) requires a vertical axis centered on the bond between two red sites or two green sites. The colors of the sites represent different charge densities. Spin ordering can also be present for an appropriate \mathbf{K} , but is not shown. Note that the bond-centered ordering naturally suggests an effective model for the spin fluctuations much like the ladder model described in the text: the spins of Fig. 2 reside on the red sites of (B) (with no spins on the green sites) and the weaker g exchange interactions (represented by the dashed lines in Fig. 2) extend across the green sites.

when both phases can be thermally excited, neither quasiparticle description is appropriate. Instead, special scale-invariance properties of the critical point have to be used to develop a new framework for finite temperature dynamics.

The availability of a large number of 2D correlated electron systems (including the high-temperature superconductors), along with the highly nontrivial theoretical framework necessary to describe them, makes this one of the most exciting research areas in condensed matter physics. As I have already noted, the increased sensitivity of future experiments, including neutron scattering, tunneling, magnetic resonance, photoemission, and optics, along with better sample preparation techniques, will surely uncover much new physics. Many interesting theoretical questions, on the classification of ground states and quantum critical points, and on the description of dynamical crossovers in their vicinity, remain open. The interplay between theory and experiment promises to be mutually beneficial, in the best traditions of physics research.

References and Notes

1. L. D. Landau and E. M. Lifshitz, *Statistical Physics* (Pergamon, Oxford, 1980).
2. S. L. Sondhi, S. M. Girvin, J. P. Carini, D. Shahar, *Rev. Mod. Phys.* **69**, 315 (1997).
3. S. Sachdev, *Quantum Phase Transitions* (Cambridge Univ. Press, Cambridge, 1999).
4. S. Sachdev and A. P. Young, *Phys. Rev. Lett.* **78**, 2220 (1997).
5. P. Pfeuty, *Ann. Phys.* **57**, 79 (1970).
6. S. Sachdev and J. Ye, *Phys. Rev. Lett.* **69**, 2411 (1992).
7. S. Chakravarty, B. I. Halperin, D. R. Nelson, *Phys. Rev. B* **39**, 2344 (1989).
8. H.-L. Lee, J. P. Carini, D. V. Baxter, W. Henderson, G. Grüner, *Science* **287**, 633 (2000).
9. J. A. Hertz, *Phys. Rev. B* **14**, 1165 (1976).
10. A. J. Millis, *Phys. Rev. B* **48**, 1783 (1993).
11. More technically, the quantum criticality described here is associated with critical points that obey hyperscaling and are below their upper critical dimension; for models with a bosonic vector order parameter, this is the case when $d + z < 4$, where z is the dynamic critical exponent ($z = 1$ for H_1).
12. N. Katoh and M. Imada, *J. Phys. Soc. Jpn.* **63**, 4529 (1994).
13. S. Tyc and B. I. Halperin, *Phys. Rev. B* **42**, 2096 (1990).
14. K. Damle and S. Sachdev, *Phys. Rev. B* **56**, 8714 (1997).
15. A. V. Chubukov, S. Sachdev, J. Ye, *Phys. Rev. B* **49**, 11919 (1994).
16. M. P. A. Fisher, G. Grinstein, S. M. Girvin, *Phys. Rev. Lett.* **64**, 587 (1990).
17. S. Sachdev and M. Vojta, <http://arxiv.org/abs/cond-mat/9908008>.
18. A. V. Chubukov and S. Sachdev, *Phys. Rev. Lett.* **71**, 169 (1993).
19. M. Vojta and S. Sachdev, *Phys. Rev. Lett.* **83**, 3916 (1999).
20. G. Aeppli, T. E. Mason, S. M. Hayden, H. A. Mook, J. Kulda, *Science* **278**, 1432 (1997).
21. T. Imai, C. P. Slichter, K. Yoshimura, K. Kosuge, *Phys. Rev. Lett.* **70**, 1002 (1993).
22. S. Chakravarty and R. Orbach, *Phys. Rev. Lett.* **64**, 224 (1990).
23. A. Sokol and D. Pines, *Phys. Rev. Lett.* **71**, 2813 (1993).
24. A. W. Hunt, P. M. Singer, K. R. Thurber, T. Imai, *Phys. Rev. Lett.* **82**, 4300 (1999).
25. S. Fujiyama, M. Takigawa, Y. Ueda, T. Suzuki, N. Yamada, *Phys. Rev. B* **60**, 9801 (1999).
26. P. Bourges, in *The Gap Symmetry and Fluctuations in High Temperature Superconductors*, J. Bok, G. Deutscher, D. Pavuna, S. A. Wolf, Eds. (Plenum, New York, 1998), pp. 349–371, <http://arxiv.org/abs/cond-mat/9901333>.
27. Y. S. Lee *et al.*, *Phys. Rev. B* **60**, 3654 (1999).
28. G. Kotliar, *Phys. Rev. B* **37**, 3664 (1988).
29. D. B. Bailey, M. Sigrist, R. B. Laughlin, *Phys. Rev. B* **55**, 15239 (1997).
30. F. Tafuri and J. R. Kirtley, <http://arxiv.org/abs/cond-mat/0003106>.
31. M. Vojta, Y. Zhang, S. Sachdev, <http://arxiv.org/abs/cond-mat/0003163>.
32. T. Valla *et al.*, *Science* **285**, 2110 (1999).
33. N. Read and S. Sachdev, *Phys. Rev. B* **42**, 4568 (1990).
34. V. N. Kotov and O. P. Sushkov, <http://arxiv.org/abs/cond-mat/9907178>.
35. V. N. Kotov, J. Oitmaa, O. P. Sushkov, W. Zheng, <http://arxiv.org/abs/cond-mat/9912228>.
36. R. R. P. Singh, W. Zheng, C. J. Hamer, J. Oitmaa, *Phys. Rev. B* **60**, 7278 (1999).
37. O. P. Sushkov, <http://arxiv.org/abs/cond-mat/0002421>.
38. J. B. Marston and I. Affleck, *Phys. Rev. B* **39**, 11538 (1989).
39. H. Schulz, *Phys. Rev. B* **39**, 2940 (1989).
40. C. Nayak, <http://arxiv.org/abs/cond-mat/0001428>.
41. D. A. Ivanov, P. A. Lee, X.-G. Wen, <http://arxiv.org/abs/cond-mat/9909431>.
42. J. M. Tranquada, N. Ichikawa, S. Uchida, *Phys. Rev. B* **59**, 14712 (1999).
43. J. Zaanen and O. Gunnarsson, *Phys. Rev. B* **40**, 7391 (1989).
44. H. Schulz, *J. Phys. (Paris)* **50**, 2833 (1989).
45. M. Kato, K. Machida, H. Nakanishi, M. Fujita, *J. Phys. Soc. Jpn.* **59**, 1047 (1990).
46. S. R. White and D. J. Scalapino, *Phys. Rev. B* **60**, R753 (1999).
47. V. J. Emery, S. A. Kivelson, J. M. Tranquada, *Proc. Natl. Acad. Sci. U.S.A.* **96**, 8814 (1999), and references therein.
48. J. M. Tranquada *et al.*, *Phys. Rev. Lett.* **78**, 338 (1997).
49. G. Baskaran and P. W. Anderson, *Phys. Rev. B* **37**, 580 (1988).
50. S. A. Kivelson, D. S. Rokhsar, J. P. Sethna, *Phys. Rev. B* **35**, 8865 (1987).
51. N. Read and S. Sachdev, *Phys. Rev. Lett.* **66**, 1773 (1991).
52. X.-G. Wen, *Phys. Rev. B* **44**, 2664 (1991).
53. S. Sachdev, *Phys. Rev. B* **45**, 389 (1992).
54. L. Balents, C. Nayak, M. P. A. Fisher, *Phys. Rev. B* **60**, 1654 (1999).
55. T. Senthil and M. P. A. Fisher, <http://arxiv.org/abs/cond-mat/9910224>.
56. J. Bobroff *et al.*, *Phys. Rev. Lett.* **83**, 4381 (1999).
57. H. F. Fong *et al.*, *Phys. Rev. Lett.* **82**, 1939 (1999).
58. S. Sachdev, C. Buragohain, M. Vojta, *Science* **286**, 2479 (1999).
59. I thank M. Fisher, C. Nayak, T. Senthil, and M. Vojta for useful discussions. This research was supported by NSF grant DMR 96-23181.

VIEWPOINT

Sources of Quantum Protection in High- T_c Superconductivity

Philip W. Anderson

The layer-structure cuprates with high superconducting transition temperatures T_c exhibit a number of anomalous electronic properties in both superconducting and normal states. These anomalies are ascribed to the existence of independent spectra of excitations for charge and for spin, signaling a collective state, a "quantum protectorate."

Laughlin and Pines (*1*) recently introduced the term "quantum protectorate" to describe certain states of quantum many-body systems with properties that are unaffected by imperfections, impurities, and thermal fluctuations. Examples are the quantum Hall effect, which can be measured to extremely high accuracy

on samples with very short mean free paths (comparable to the electron wavelength), and flux quantization in superconductors, which is independent of imperfections and scattering. A simpler example is the rigidity and dimensional stability of crystalline solids evinced by scanning tunneling microscopy. The source of quantum protection is likely to be a collective state of the quantum field, in which the individual particles are sufficiently tightly coupled that elementary excitations no

longer involve just a few particles, but are collective excitations of the whole system. As a result, macroscopic behavior is mostly determined by overall conservation laws.

Here, I discuss experimental evidence which shows that the metallic states of high-transition temperature (T_c) cuprate superconductors are a quantum protectorate. I propose that this collective state involves the phenomenon of charge-spin separation and give indications why such a state should be a quantum protectorate.

Experimental Evidence

We may define four regions of the generic cuprate phase diagram (Fig. 1): the "normal" metallic state near optimal doping, phase I,

Joseph Henry Laboratories of Physics, Princeton University, Princeton, NJ 08544, USA. E-mail: pwa@puppp.princeton.edu